Particle-in-Cell Modeling of the Nanosecond Field Emission Driven Discharge in Pressurized Hydrogen

Dmitry Levko,[1] Shurik Yatom,[2] and Yakov E. Krasik[3]

[1]Department of Aerospace Engineering and Engineering Mechanics, The University of Texas at Austin, Austin, TX 78712, USA

[2]Princeton Plasma Physics Laboratory, Princeton, NJ 08543, USA

[3]Department of Physics, Technion, 32000 Haifa, Israel

The high-voltage field-emission driven nanosecond discharge in pressurized hydrogen is studied using the one-dimensional Particle-in-Cell Monte Carlo collisions model. It is obtained that the main part of the field-emitted electrons becomes runaway in the thin cathode sheath. These runaway electrons propagate the entire cathode-anode gap, creating rather dense (~10^{12} cm^{-3}) seeding plasma. In addition, these electrons initiate a streamer propagating through this background plasma with a speed ~30% of the speed of light. Such a high streamer speed allows the self-acceleration mechanism of runaway electrons present between the streamer head and the anode to be realized. As a consequence, the energy of runaway electrons exceeds the cathode-anode gap voltage. In addition, the influence of the field emission switching-off time is analyzed. It is obtained that this time significantly influences the discharge dynamics.

I. Introduction

The research of high-voltage (HV) nanosecond (ns) pulse discharges in pressurized gases has attracted considerable attention since the 1960's[1-4] because of the interesting phenomena involved and their important applications, such as plasma assisted ignition and combustion, pulsed gaseous lasers, and the generation of electron beams and x-rays.[4]

Depending on the voltage applied, different physical phenomena are involved and govern this type of pulse discharge.[1-4] At very high voltages (>100 kV), the electric field at the cathode surface, having micro-protrusions, reaches ~10^9 V/m, which is sufficient for intense electron field emission (FE). Numerous experimental and numerical modeling studies[5-21] have shown that at such an extremely high electric field, one can obtain runaway electrons (RAE), i.e., electrons that acquire more energy during their acceleration by an electric field along a mean free path than they lose in inelastic collisions with neutrals or ions. RAE propagate the entire cathode-anode (CA) gap, experiencing only a few collisions and generating a seeding (secondary) electron background. This seed allows the bridging of the CA gap by dense plasma on the sub-ns timescale, which is impossible without RAE.

In order to obtain RAE generation, one needs to apply an electric field exceeding the threshold value E_{cr}, which depends on the background gas type and its pressure.[1-4] At normal atmospheric pressure, for many gases this electric field varies in the range 1-5×10^7 V/m. Thus, in the case where the electric field at the cathode surface is ~10^9 V/m, the main part of FE electrons become RAE, obtaining energy >>10 keV in the vicinity of the cathode.[17] However, depending on the anode and cathode electrodes geometry, CA gap, and the pressure and type of the gas, these electrons do not necessarily continue to be RAE during their propagation toward the anode. Only if the electric field is >E_{cr}, do high-energy electrons continue to accelerate, i.e., remain

RAE. However, if the electric field in the CA gap is significantly smaller than E_{cr}, a significant part of these high-energy electrons' energy can be dissipated during their propagation toward the anode through elastic and inelastic collisions.[5]

HV discharge in an air-filled diode at atmospheric and elevated pressures in a non-uniform electric field in a ns-timescale has been studied in many laboratories worldwide.[1-16,20-21] For, instance, the results reported in Ref. 16 showed that the beginning of the electron generation precedes the appearance of light emission at the blade-type cathode edge, indicating that RAE generation occurs via FE prior to the formation of the cathode explosive plasma. Furthermore, it was found that the measured RAE energy spectrum shows that the maximal energy of electrons arriving at the anode is $\leq e\varphi_{CA}$, where e is the electron charge and $\varphi_{CA} \approx$120 kV is the applied voltage, and this spectrum can be fitted with Maxwell distribution for electrons with energies ≥20 keV. The discharge has the form of separate plasma channels, originating at the cathode edge, and the light emission front propagates toward the anode at a velocity of ~10^9 cm/s, corresponding to the velocity of electrons with energy of ~300 eV, i.e., with sufficient energy to allow ionization and excitation processes. This propagation velocity decreases with an increase in the gas pressure and the CA gap length. At atmospheric gas pressure, these plasma channels take the form of diffusive jets and this form is changed to that of contracted channels as the pressure increases to $\geq 2\times10^5$ Pa.

An interesting observation about the electrons with anomalously high energy was reported and discussed, for instance, in Refs. 1-4 and 22-24. These electrons are the electrons having energy that exceeds the value $e\varphi_{max}$, where φ_{max} is the maximum amplitude of the voltage pulse applied to the cathode. The most probable explanation of this phenomenon is "anomalous"

electron generation due to the self-acceleration mechanism, as suggested by Askarayn[25] (see Sec. IV).

The results presented in this paper continue those of the studies reported in Refs. 16 and 17. In the present study, the self-consistent one-dimensional Particle-in-Cell Monte Carlo collisions (1D PIC/MCC) model was used with more accurate treatment of FE electrons. This treatment allows us to obtain the results that were only speculated in earlier research. It should also be noted that we focused only on the streamer discharges, the time- and space evolution of which is governed by FE electrons opposite to the streamers propagating through the natural electron background, which was analyzed in recently published review papers (see Refs. 26-28 and references therein).

II. Numerical model

In order to study HV high-pressure discharge, we updated the model developed in Ref. 17. This is a 1D PIC/MCC model in cylindrical coordinates considering a coaxial diode. The cathode is the inner rod made of copper with radius r_C ~3 μm and the anode is the outer cylinder having radius r_A = 1 cm. The anode is grounded, while the cathode voltage is changed in time as $U_C = U_0 \cdot \sin(2\pi t/T)$, where U_0 = -100 kV and T = 10 ns**, i.e. the voltage rise time is $\boldsymbol{T/4}$ = 2.5 ns**. **This voltage temporal dependence was used to fit the voltage waveforms obtained in experimental research[16] [see Fig. 3(g) in Ref. 16].** The diode is filled with molecular hydrogen (H_2) at a pressure of $P = 2\times10^5$ Pa and temperature T_g =300 K.

The model accounts for the electron-neutral momentum transfer collisions, excitation of the first three electronic levels of H_2, and excitation of rotational and vibrational levels, dissociation, and ionization **(see Fig. 1)**. If ionization occurs, one electron-ion (H_2^+) pair is added to the simulation domain. Note that excitation and dissociation collisions do not lead to the

generation of new species. These collisions lead only to the electron energy losses that must be considered for the accurate treatment of the total electron energy losses. **For electron-H_2 ionization cross sections the NIST database was used.**[29] The cross sections of **other** collisions **were** taken from Biagi's database.[30] The collisions between electrons and the possible products of dissociation of H_2 (e.g., H) were not considered in the present model.

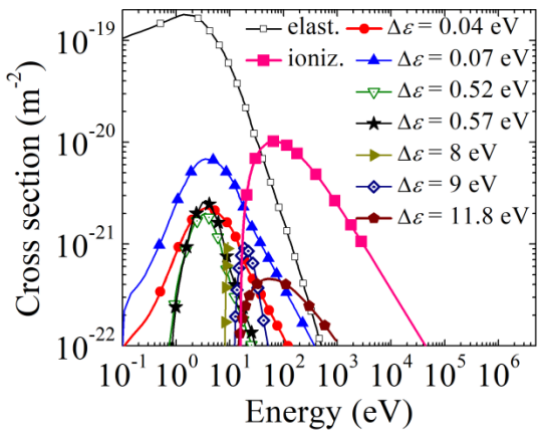

FIG. 1. Electron-H_2 cross sections used in 1D PIC/MCC model.

In the model, the electron FE from the cathode is considered using the Fowler-Nordheim (FN) equation[31]

$$j_{FN} = 6.2 \times 10^{-6} \frac{(\varepsilon_F/\varphi)^{1/2}(E)^2}{\varepsilon_F+\varphi} \cdot \exp\left[-\frac{6.85\times10^7\varphi^{3/2}\xi}{E}\right]. \quad (1)$$

Here, $\varepsilon_F = 7.0$ eV is the Fermi energy, E is the electric field at the cathode surface, and φ = 4.4 eV is the work function for the cathode made of copper.[31] ξ is the correction factor, which depends on both E and φ.[31]

In the model considered here, the cathode material is taken into account only through the work function φ. For many materials, work function varies in the range ~2-5 eV[32] which can significantly influence the discharge dynamics (see, for instance, discussion in Refs. 33-34). Namely, the decrease of the cathode material work function will decrease the time when the noticeable FE is obtained (see discussion in Section III). This, in turn,

will influence the energy of RAE and can change the discharge dynamics.

The exponential dependence of the FE current on the electric field [Eq. (1)] renders the modeling of high-pressure discharges driven by FE very challenging. Indeed, the discharge, ignited by a small FE current, very quickly transfers to a dense plasma generated in the CA gap, and a thin non-neutral sheath is formed between the plasma boundary and cathode surface. The potential drop on this sheath, depending of the plasma resistivity, can reach a significant part of the voltage applied to the CA gap. The latter leads to an increase of a few orders of magnitude in the FE current due to the increase in the electric field at the cathode surface. For instance, in the conditions of this study, the FE current density varies in the range 10^6-10^{10} A/m^2. This temporal and spatial evolution of the FE process, plasma, and sheath formation is accompanied by a variation in the plasma density in the range 10^9-10^{23} m^{-3}. To cover such a wide range of density with the constant weight of "macro"-particles (i.e., the number of real particles in each computational particle), one needs to use ~10^9 "macro"-particles even in 1D simulation. In order to overcome this computational restriction, we implemented an algorithm for merging "macro"-particles (for details, see Ref. **35**) to keep the overall "macro"-particle number below a specified threshold. In this study, this threshold was set at 10^6 for each species. By this method, two "macro"-particles of the same type neighboring in the phase space are merged. The velocity and position of the new "macro"-particle are defined as the average values of the velocities and positions of the two merged particles.

However, this merging algorithm is not effective for energetic electrons generated as a part of the FE electrons, because the number of these energetic electrons is significantly smaller than that of the secondary electrons generated in the CA gap. These energetic electrons belong to the tail of the electron energy distribution function, and the velocity of their neighbors in phase

space can be considerably smaller. Hence, the merging of energetic and "cold" plasma electrons, the energy of which is only a few tens of eV, leads to the numerical “cooling” of the former. To overcome this artificial cooling, FE and plasma electrons were considered as two different types of "macro"-particles. **Note that the plasma electrons are all electrons generated in the gap due to the gas ionization.**

To facilitate the model’s implementation, FE electrons were not divided into fast and slow groups, because, as shown in the following, all FE electrons finally become RAE. The weight of FE electrons w_{FE} was kept constant during the simulation; i.e., the merging algorithm was not applied to these particles. Namely, the weight of FE “macro”-particles was selected to keep their total number below the set threshold value of 10^6. The weight of plasma electron macro-particles w_p was varied in time; i.e., they were merged during the simulation. For brevity, hereinafter, FE and plasma electrons are considered to represent the corresponding “macro”-particles. The collisions for both groups of electrons were modeled using the same Monte Carlo algorithm. If the electron (FE or plasma) produces ionizing collisions with the H_2 molecules, a new electron/ion pair was added to the simulation domain. Because of the difference in weights for the FE and plasma electrons, an additional source term $S_i(x)$ was introduced. This source accounts for the ionization events produced only by the FE electrons. If the FE electron experiences an ionizing collision, one electron with the weight w_{FE} is added to $S_i(x)$. In each time step, the function $S_i(x)$ was checked and if the condition $S_i(x)/w_p \geq 1$ was satisfied, the number $\mathrm{int}(S_i(x)/w_p)$ of electrons was added to the plasma electrons. The space step used in this model is $\Delta x = 0.2$ μm, allowing the resolution of the parameters of the spatial gradients inside the CA, including the cathode sheath. The time step, $\Delta t = 10^{-15}$ s, is dictated by the Courant condition.

III. Results and discussion

A. Discharge dynamics

This subsection presents the results of the 1D PIC/MCC simulations obtained for H_2 gas at pressure P = 2×10^5 Pa. For a cathode radius of 3 μm, the FE current reaches the value ~10^6 A/m^2 at $t \approx$ 1.3 ns, which leads to the emission of the first "macro"-particles to the CA gap. At this time, the applied voltage reaches 73 kV and the electric field at the cathode surface is $E_C \approx$ 2.8×10^9 V/m (see Fig. **2**). This electric field significantly exceeds the E_{cr}~ 6×10^7 V/m necessary for the electrons to run away in H_2 gas at P = 2×10^5 Pa. The latter results in FE electrons becoming runaway almost immediately after their injection into the CA gap, acquiring energy >1 keV at a distance of a few microns from the cathode. These energetic electrons also generate electron/ion pairs during their acceleration toward the anode. The total electron-neutral collision cross section of 2-keV electrons in H_2 gas is ~2×10^{-21} m^2, resulting in the mean free path of these electrons in H_2 gas $\lambda \sim$ 10 μm. One can see that, at r = 13 μm, the electric field $E(r) = U_C/[r \cdot ln(r_A/r_C)]$ decreases ~3.6 times, but its value is still significantly larger than E_{cr}. Only at radii >0.8 mm does the electric field become smaller than E_{cr} . Hence, the plasma electrons generated in the vicinity of the cathode also become RAE, although the energy of these electrons is smaller than that of FE electrons.

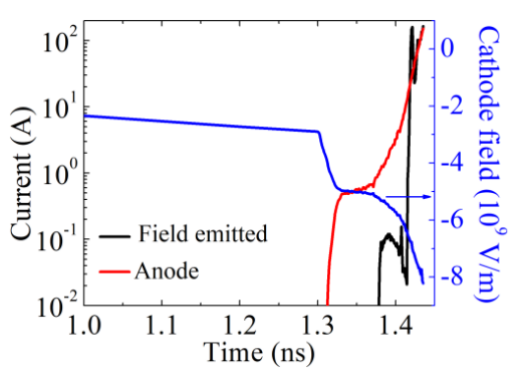

FIG. **2**. Time evolution of the field emission current and electron current through the anode, and electric field at the cathode.

The simulation results show that, in the CA gap, ~99% of the plasma charged particles is generated by the plasma electrons and only ~1% is generated by the FE electrons. This result is related to the significantly larger number density of plasma electrons, $\boldsymbol{n_e}$, than of FE electrons, $\boldsymbol{n_{RAE}}$ **(**$\boldsymbol{n_{RAE}/n_e}$**~ 0.01),** as well as to the fact that the ionization frequency ν_i of plasma electrons having energy $\varepsilon_e \ll 100$ eV is much larger than ν_i of FE electrons with energy $\varepsilon_e \gg 1$ keV.

Figure **3** shows the space evolution of the electron density and potential at different times of the discharge development. Figure **3**(a) shows that at $t \approx 1.3$ ns the density of the plasma generated in the vicinity of the cathode reaches $n_e \sim 10^{14}$ cm^{-3}. This plasma screens the applied electric field leading to the formation of a thin (a few microns) cathode sheath [Fig. **3**(c)]. This results in an increase in the electric field at the cathode surface, and respectively, in a significant increase in the FE current (Fig. **2**). The latter, in its turn, leads to a further increase in the plasma electron density. Figure **3**(a) shows that at $t \approx 1.4$ ns the plasma density reaches $n_e \sim 10^{16}$ cm^{-3} in the cathode vicinity. The sheath thickness obtained at this time is $l_{sh} \sim 20$ µm and the sheath voltage is $U_{sh} \sim 25$ kV.

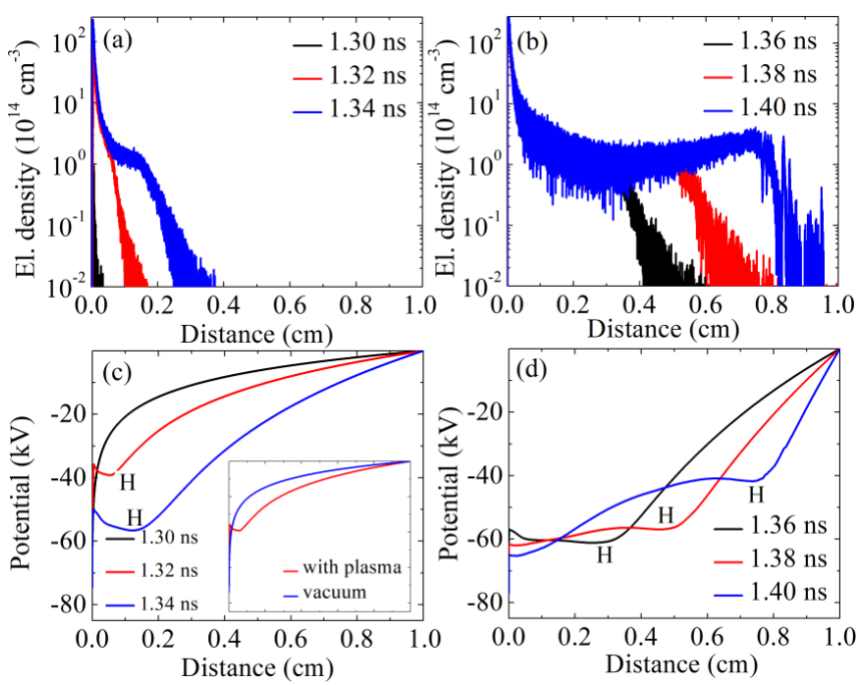

FIG. **3**. (a, b) Electron density and (c, d) potential obtained at different times; $P = 2\times10^5$ Pa. The insert in (c) shows the potential distribution with and without plasma at $t = 1.32$ ns. H denotes the position of the streamer head.

Figure **4**(a) presents the energy phase space of emitted electrons at 1.36 ns. One can see that the FE electrons are accelerated in the sheath, acquiring energy up to $\sim eU_{sh}$; i.e., these electrons become RAE. The electron-H_2 ionization cross section of 20-keV electrons is $\sigma_{ion}\sim$ 9×10^{-23} m^2. The mean free path of these electrons is $\lambda\sim$ 100 μm and the ionization collision frequency is $\nu_{ion}\sim$ 3.6×10^{11} s^{-1}. These 20-keV electrons propagate in the electric field $E\sim$ 10^7 V/m. The energy gained by 20-keV electrons between two consecutive ionization collisions can be estimated as $\Delta\varepsilon = q_e^2E^2/(2m_e\nu_{ion}^2) \approx$ 66 eV which significantly exceeds the ionization energy of an H_2 molecule (15.4 eV). Thus, the FE electrons that become runaway in the cathode sheath propagate the entire CA gap, remaining RAE.

One can conclude from Fig. **3**(a) that the FE-driven discharge can be described using the commonly accepted model[31] of the anode-directed streamer [see Fig. **3**(b,d)]. Following Ref. **31**, an anode-directed streamer is defined as a quasi-neutral plasma jet (density ~10^{13}-10^{15} m^{-3}) acquiring a large part of the cathode potential and propagating toward the anode. A high-intensity electric field is obtained only at the streamer head, where the plasma quasi-neutrality is violated because of space separation between the fast electrons and ions at that location. At the beginning of FE, i.e., when the first FE electrons become accounted for in the simulations, a low-density (<10^{12} cm^{-3}) plasma is formed in the vicinity of the cathode, transforming very quickly to the propagating streamer. A large part of FE electrons becomes RAE, experiencing very few ionization collisions during their propagation toward the anode. Nevertheless, these ionization collisions lead to the formation of seeded electrons in front of the streamer head (see Fig. **4**) with a density of ~10^{12} cm^{-3}, which significantly exceeds the natural background electron density

(~10^3 cm^{-3}) commonly assumed in streamer models.[31] This result, namely, the increasing streamer velocity for increasing density of the seeding background, qualitatively agrees with the theory developed in Ref. **36**.

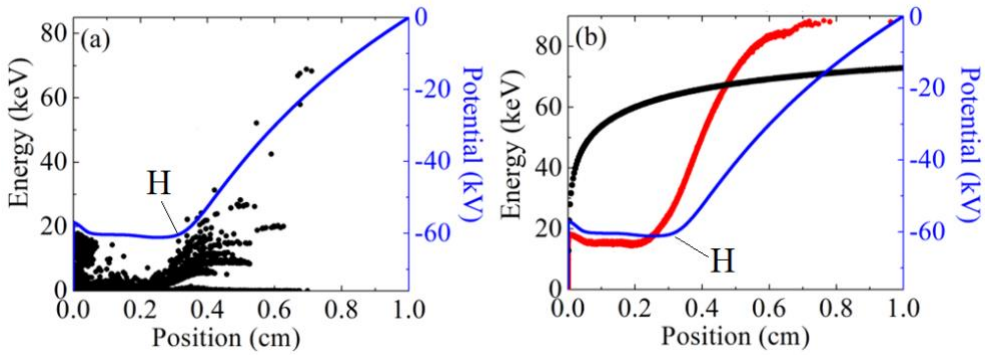

FIG. **4**. (a) Energy phase space of plasma electrons and (b) phase space of field emission (FE) at t =1.36 ns; P = 2×10^5 Pa. Blue line shows the distribution of potential at the same time. Black dots in Fig. 3(b) show the energy phase space of FE electrons for vacuum conditions.

A high electric field (~1-2×10^7 V/m) is obtained at the streamer head, which we determined as points H in Figs. **3**(c, d), where the maximal negative potential is realized. This electric field accelerates seeded electrons at those locations to energies exceeding the ionization threshold of H_2, thus supporting the streamer propagation. Since the density of seeded electrons is ~10^{12} cm^{-3}, the streamer obtained during the discharge supported by FE and, respectively, by these seeded electrons, propagates significantly faster than that considered**,** for instance, in Ref. **31**. One can see in Fig. **3** that the streamer propagates a distance ~0.8 cm during 100 ps, resulting in a streamer average velocity v_{fr}~ 8×10^7 m/s. Here, let us note that the average velocity of the conventional anode-directed streamer is only ~10^5 m/s.[31]

Figure **4** shows the typical energy phase spaces of the plasma and FE electrons at t = 1.36 ns. One can see in Fig. **4**(a) that part of the plasma electrons also becomes RAE. These plasma electrons were generated in the cathode sheath due to the gas ionization by FE electrons. In addition, the electric field at point H [see Fig. **4**(a)] is ≤2×10^7 V/m; i.e., it is significantly smaller

than the value of E_{cr} necessary for RAE generation in H_2. Thus, the streamer head cannot be considered a source of RAE generation under the given conditions for H_2 gas.

In Fig. **4**(b), one can see that the energy of FE electrons $\varepsilon_{e,em}$ reaches ~88 keV, while the cathode potential at t =1.36 ns is only -75.4 kV, i.e., $\varepsilon_{e,em} > e|U_C|$. Let us note that the number of such "anomalous" electrons is ~0.1% of the total number of electrons obtained at that time in the CA gap. The anomalous high energy of FE electrons can be explained by the self-acceleration mechanism suggested by Askar'yan.[25] The simulation results show that, because of the high density (~10^{12} cm^{-3}) of seed electrons generated by RAE in front of the streamer head, one obtains streamer propagation toward the anode with $v_{fr}\sim$ 8×10^7 m/s and an electric field at the streamer head of ~10^7 V/m. In the frame of the fast propagating streamer, the RAE present between the streamer head and the anode acquire additional energy (with respect to $e|U_C|$), which can reach tens of keV. Let us note that sometimes in the literature such a fast propagating streamer is called an ionization wave.

Figure **5** shows the electron density and potential distributions and the energy phase spaces of plasma and FE electrons obtained at t = 1.42 ns when the streamer bridges the CA gap. At that time, the cathode sheath width is $l_{sh}\sim$ 1.5 μm with a voltage drop of ~4.6 kV and the plasma density in the vicinity of the cathode sheath reaches ~10^{17} cm^{-3}. One can see that an electric field ~7×10^6 V/m is present in the plasma [see Fig. **5**(a)], indicating the high resistivity of the plasma. A similar electric field value of ~3×10^6 V/m in the plasma channel was recently measured in the HV ns-timescale discharge in H_2 gas at a pressure of 2×10^5 Pa.[16]

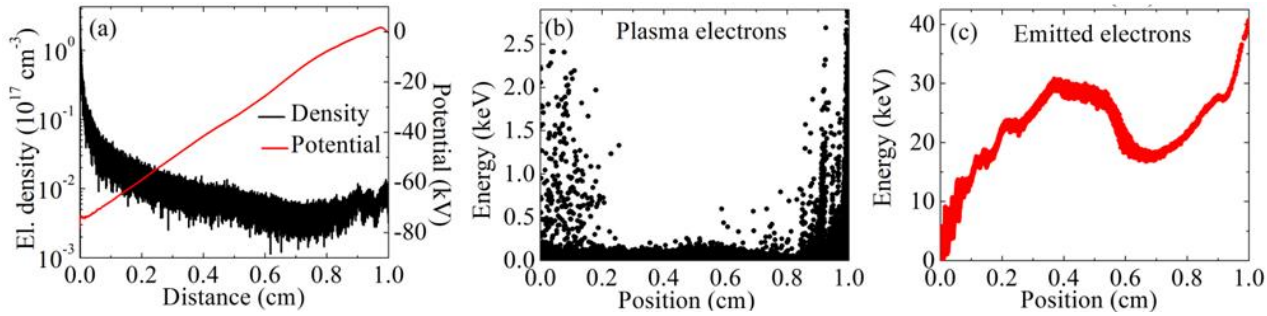

FIG. **5**. (a) Electron density and potential, (b) phase space of plasma electrons, and (c) energy phase space of field emission electrons obtained at t = 1.42 ns.

The energy phase space of FE electrons [Fig. **5**(c)] shows that these electrons can be considered RAE, although their energy in the anode vicinity is smaller than $e|U_C|$ [U_C = -77.9 kV, Fig. 4(a)]. The energy of FE electrons entering the plasma bulk from the cathode sheath is only ~4.6 keV, but it is sufficient for these electrons to remain in the acceleration in the weaker electric field obtained in the plasma bulk (~7×10^6 V/m).

The energy phase space of plasma electrons shows the presence of two groups of energetic (up to several keV) electrons located close to the cathode and anode [see Fig. **5**(b)]. Close to the anode are the electrons that became RAE before the streamer bridged the CA gap, whereas close to the cathode are energetic electrons generated in the cathode sheath by FE electrons. The latter cannot be considered RAE, despite the fact that these electrons enter the plasma bulk with an energy ~2.5 keV. The latter is explained by the insignificant electric field in the plasma bulk, which is smaller than E_{cr}. Thus, almost all the energy of these energetic electrons is dissipated during their propagation toward the anode.

B. Role of the FE electrons in streamer propagation dynamics

In order to understand the role of FE electrons in the dynamics of streamer propagation and the distributions of the plasma density and potential in the CA gap, additional PIC/MCC simulations were performed. In these simulations, the FE was artificially switched off with a time delay τ with respect to the beginning of electron emission. It is understood that in the

experimental conditions, FE will be transferred to explosive emission plasma formation. However, because of the fast (up to ~5×10^4 m/s) expansion of the plasma acquiring cathode potential, the electric field at the plasma boundary decreases quickly below E_{cr} and the electrons emitted from the boundary of this plasma cannot be considered RAE.

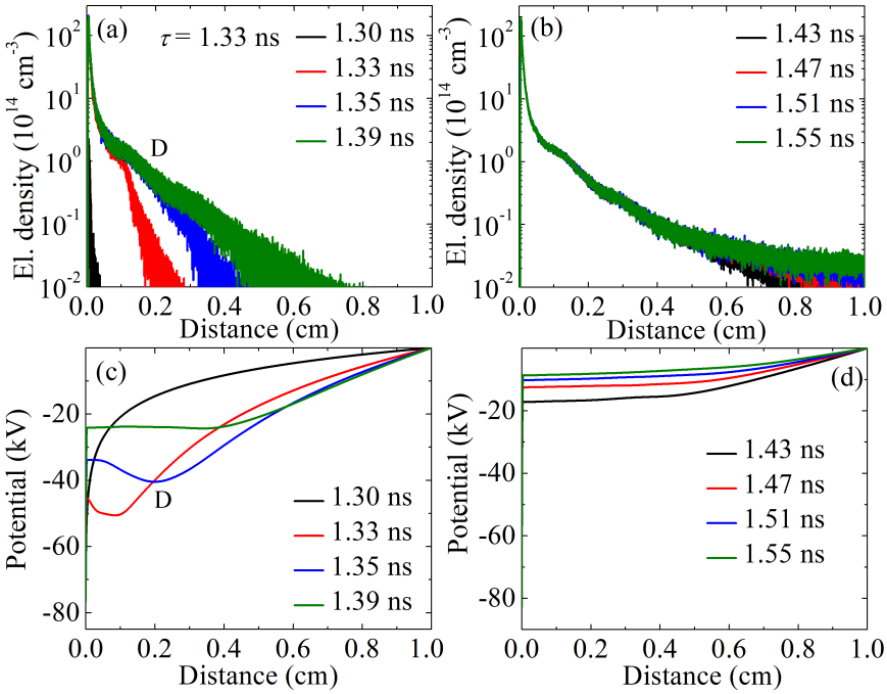

FIG. **6**. (a,b) Electron density, and (c, d) potential distributions obtained at different times; H_2 gas pressure is of 2×10^5 Pa, field emission is switched-off at τ = 1.33 ns.

Figure **6** shows the electron density and potential distributions at different times with respect to τ = 1.33 ns. At t = 1.33 ns [see Fig. **3**(a)], the streamer propagates ~0.2 cm and the anode current reaches ~0.8 A (see Fig. **2**). At that time, one obtains that between the dense (>10^{14} cm^{-3}) plasma [see point D in Figs. **6**(a) and (c)] and anode there is a plasma (0.1 cm < r < 0.3 cm) formed by the RAE and plasma electrons prior to the FE switch-off with density ≤10^{13} cm^{-3}. Later in time, one obtains [see Fig. **6**(b)] rather gradual plasma formation toward the anode. Indeed, a comparison of the distributions presented in Figs. **3** and **6** shows that after the FE switch-off, there is no fast propagation of the streamer as compared with the case of continuous FE of electrons. The latter is explained by the fact that the conditions necessary for self-

consistent fast streamer propagation are not satisfied at τ = 1.33 ns. Indeed, at this time the electric field at the "head" of the streamer is ~10^7 V/m, i.e., it is smaller than the electric field necessary for the H_2 breakdown by means of the streamer. In addition, at this time only a small number of RAE electrons cross the CA gap and therefore the density of the seeded electrons is not sufficient to obtain a fast propagating streamer.

Figure **6**(d) shows the potential distributions at t > 1.43 ns, when the CA gap is bridged by the plasma with density >10^{13} cm^{-3}. At these times, there are three regions with different plasma density and potential distribution, namely, a thin cathode sheath ($l_{sh}\sim$ 30 μm), where ions' acceleration toward the cathode occurs, the region of quasi-neutral plasma, where the electric field is ~10^5 V/m, and the anode layer with an electric field of ~10^6 V/m. The anode layer formation is dictated by the current continuity, since the plasma density in the vicinity of the cathode sheath edge is ~10^3 times larger than that in the anode vicinity [see Fig. **6**(b)].

The energy phase spaces of FE electrons prior to and after FE termination at τ = 1.33 ns are shown in Fig. **7**. One can see that the energy of FE electrons does not exceed $e|U_C|$, as was obtained with continuous electron FE. Moreover, at 0.14 ns after the FE is switched off, the energy of electrons reaching the anode already does not exceed 25% of $e|U_C|$. The latter is explained by the drastic decrease in the electric field in the CA gap [see Fig. **6**(d)], resulting in that FE electrons cannot be now considered RAE.

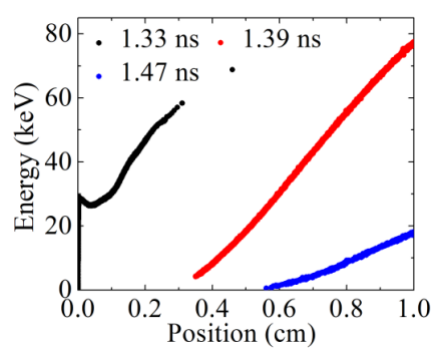

FIG. **7**. Phase space of field emission (FE) electrons obtained at three different times; H_2 gas pressure is

of 2×10^5 Pa, FE is switched off at τ = 1.33 ns.

The simulation results for electron density and potential distributions obtained at different times for τ = 1.4 ns are shown in Fig. **8**. One can see that a 0.07 ns time delay in switch-off of the FE as compared with the previous case changes drastically the discharge dynamics; namely, one can clearly see the propagation of the fast streamer, similarly to the case of continuous electron FE.

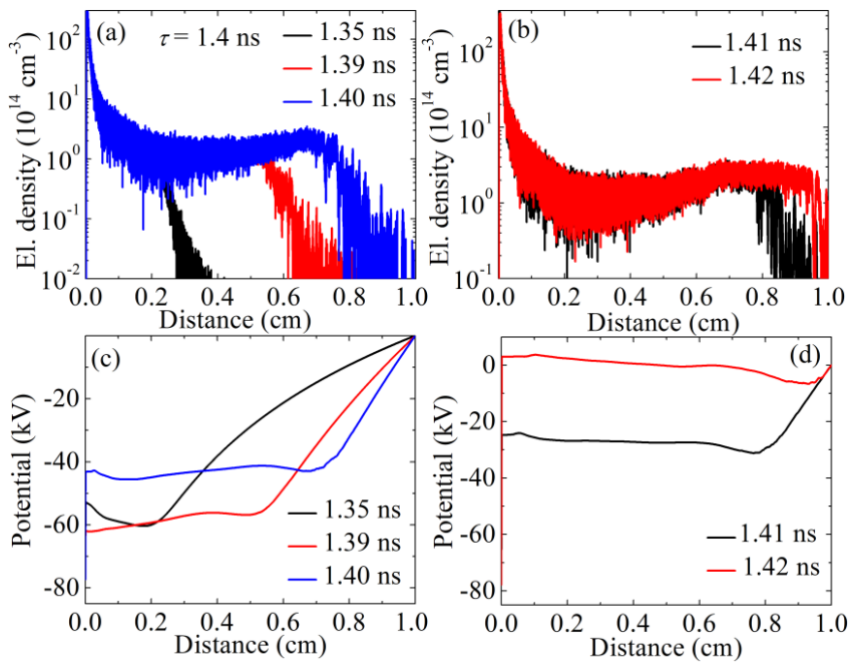

FIG. **8**. (a,b) Electron density, and (c, d) potential distributions obtained at different times; H_2 gas pressure is of 2×10^5 Pa, field emission is switched off at τ = 1.4 ns.

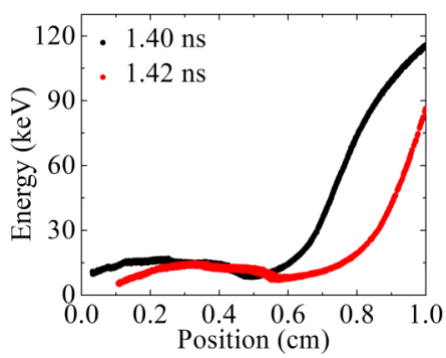

FIG. **9**. Phase space of field emission (FE) electrons obtained at two different times; H_2 gas pressure is of 2×10^5 Pa, FE is switched off at τ = 1.4 ns.

Such a significant sensitivity to the value of τ formation and the fast propagation of the

streamer is related to the number of FE electrons emitted prior to the switch-off instant. Indeed, the anode current reaches 2 A at t = 1.4 ns (see Fig. **2**), which is 2.5 times larger than the anode current obtained at t = 1.33 ns. The latter is related to the significantly larger number of FE electrons injected into the CA gap prior to the FE switch-off for τ = 1.4 ns than for τ = 1.33 ns and, respectively larger number of RAE present in the CA and producing larger density of seeded electrons across the entire CA gap (see Figs. **7** and **9**). However, even at τ = 1.4 ns, when one obtains fast streamer propagation after FE termination, the energy of FE reaching the anode does not exceed $e|U_C|$ because of the significantly smaller electric field at the streamer head.

IV. Summary

High-voltage nanosecond discharge in hydrogen was studied using the one-dimensional Particle-in-Cell Monte Carlo collisions model. The discharge was driven by the electron field emission from the small-curvature cathode.

It was obtained that the main part of FE electrons becomes runaway in the thin cathode sheath. These runaway electrons propagate the entire cathode-anode gap, creating rather dense (~10^{12} cm^{-3}) seeding plasma electrons. Then, the discharge develops in the form of a streamer propagating through this background plasma with the velocity of ~10^8 m/s. This allows runaway electrons to acquire more energy than $e|U_C|$ due to acceleration by the electric field at the head of the streamer. The number of these anomalous energetic electrons does not exceed 0.1% of the total number of FE electrons. The peak plasma density ~10^{17} cm^{-3} was obtained in the vicinity of the cathode, while the electric field in the plasma channel was ~7×10^6 V/m.

Finally, the influence of the FE switch-off time was analyzed. It was obtained that an early switch-off stops the ionization wave propagation. The bridging of the cathode-anode gap was realized by means of the RAE remained in the gap. However, a late FE switch-off does not

stop the ionization wave propagation. This was explained by the injection of the large number of electrons from the cathode prior to the FE switch-off. As a consequence, a large number of RAE electrons was present in the cathode-anode gap, which drives the ionization wave propagation.

References

[1] L. P. Babich, T. V. Loiko and V. A. Tsukerman, Physics – Uspekhi **33,** 521 (1990).

[2] V. F. Tarasenko and S. I. Yakovlenko, Physics – Uspekhi **47,** 887 (2004).

[3] L. P. Babich, *High-Energy Phenomena in Electric Discharges* (Futurepast, Arlington, Virginia, 2003), Vol. 2.

[4] *Runaway Electrons Preionized Diffuse Discharges*, editor V. F. Tarasenko (Nova Publishers, New York, 2015).

[5] Yu. D. Korolev and G. A. Mesyats, *The Physics of Pulse Breakdown* (Nauka, Moscow, 1991 in Russian).

[6] G. A. Mesyats, M. I. Yalandin, K. A. Sharypov, V. G. Shpak and S. A. Shunailov, IEEE Trans. on Plasma Science **36,** 2497 (2008).

[7] V. F. Tarasenko, E. Kh. Baksht, A. G. Burachenko, I. D. Kostyrya, M. I. Lomaev and D. V. Rybka, IEEE Trans. on Plasma Science **38,** 741 (2010).

[8] G. A. Mesyats and M. I. Yalandin, IEEE Trans. on Plasma Science **37,** 785 (2009).

[9] S. Ya. Belomyttsev, I. V. Romanchenko, V. V. Ryzhov and V. A. Shklyaev, Tech. Phys. Lett. **34,** 367 (2008).

[10] V. A. Shklyaev and V. V. Ryzhov, Tech. Phys. Letters **37,** 72 (2011).

[11] S. N. Ivanov, V. V. Lisenkov and V. G. Shpak, J. Phys. D: Appl. Phys. **43,** 315204 (2010).

[12] T. Shao, V.F. Tarasenko, Ch. Zhang, E. Kh. Baksht, D. Zhang, M. V. Erofeev, Ch. Ren, Y. V. Shutko and P. Yan, J. Appl. Phys. **113,** 093301 (2013).

[13] T. Shao, V. F. Tarasenko, Ch. Zhang, D. S. Beloplotov, W. Yang, M. I. Lomaev, Z. Zhou, D. A. Sorokin and P. Yan, Phys. Lett. A. **378,** 1828 (2014).

[14] S. Yatom and Y. E. Krasik, J. Phys. D: Appl. Phys. **47**, 215202 (2014).

[15] S. Yatom, V. Vekselman, J. Z. Gleizer and Ya. E. Krasik, J. Appl. Phys. **109,** 073312

(2011).

[16] S. Yatom, S. Tskhai and Ya. E. Krasik, Phys. Rev. Lett. **111,** 255001 (2013).

[17] D. Levko, S. Yatom, V. Vekselman, J. Z. Gleizer, V. Tz. Gurovich and Ya. E. Krasik, J. Appl. Phys. **111,** 013303 (2012).

[18] D. Levko and L. L. Raja, J. Appl. Phys. **119,** 153301 (2016).

[19] N. Yu. Babaeva and G. V. Naidis, Phys. Plasmas **23,** 083527 (2016).

[20] E. Marode, Ph. Dessante and P. Tardiveau, Plasma Source Sci. Technol. **25,** 064004 (2016).

[21] N. Yu. Babaeva, Ch. Zhang, J. Qiu, X. Hou, V. F. Tarasenko and T. Shao, Plasma Source Sci. Technol. **26,** 085008 (2017).

[22] V. F. Tarasenko, E. K. Baksht, D. V. Beloplotov, A. G. Burachenko, I. D. Kostyrya, M. I. Lomaev, D. V. Rybka and D. A. Sorokin, JETP Letters **102,** 350 (2015).

[23] A. M. Boichenko, Tech. Phys. **56,** 317 (2011).

[24] L. P. Babich and T. V. Loiko, JETP Letters **101,** 735 (2015).

[25] G. A. Askaryan, JETP Lett. **1,** 44 (1965).

[26] J. Qin and V. P. Pasko, J. Phys. D: Appl. Phys. **47,** 435202 (2014).

[27] C. Li, J. Teunissen, M. Nool, W. Hundsdorfer and U. Ebert, Plasma Source Sci. Technol. **21,** 055019 (2012).

[28] D. V. Rose, D. R. Welch, R. E. Clark, C. Thoma, W. R. Zimmerman, N. Bruner, P. K. Rambo, and B. W. Atherton, Phys. Plasmas **18,** 093501 (2011).

[29] Electron-H_2 ionization cross section: https://physics.nist.gov/cgi-bin/Ionization/table.pl?ionization=H2

[**30**] Biagi database: www.lxcat.net/Biagi

[**31**] Yu. P. Raizer, *Gas Discharge Physics* (Springer-Verlag, Berlin, 1991).

[32] I. K. Kikoin, Tables of Physical Quantities (Atomizdat, Moscow, 1976) (in Russian)

[33] C. Zhang, V. F. Tarasenko, T. Shao, E. Kh. Baksht, A. G. Burachenko, P. Yan, and I. D. Kostyray, Laser and Particle Beams 31, 353 (2013).

[34] E. Kh. Baksht, A. G. Burachenko, V. F. Tarasenko, Tech. Phys. 60, 1645 (2015).

[**35**] C. H. Shon, H.J. Lee and J. K. Lee, Comput. Phys.Commun.**141,** 322 (2001).

[**36**] S. I. Yakovlenko, Technical Physics **49,** 1150 (2004).